This article has been accepted for publication in a future issue of this journal, but has not been fully edited. Content may change prior to final publication. Citation information: DOI 10.1109/TPWRD.2018.2889895, IEEE Transactions on Power Delivery

Protection Method for Radial Distribution Systems with DG Using Local Voltage Measurements

Sadegh Jamali, and Hossein Borhani-Bahabadi

***Abstract*—This paper presents a voltage-based protection method for distribution systems with distributed generation (DG). Considering the fact that any system fault is associated with a voltage dip at the faulted line ends, a novel protection relay characteristic is formulated from an extensive analysis of voltage behavior during fault conditions. The proposed method is independent of type, size and location of DG units, as well as grid-connected or islanded (stand-alone) mode of operation of the distribution system. Moreover, the method is communication-less and uses only the local voltage magnitude to determine the relay operating time, hence a low-cost protection method is provided. A threshold voltage level is defined outside the nominal voltage range. However, if under a fault condition the voltage dip is still within the nominal range, a current starter is used to trigger the relay. The effectiveness of the proposed method is verified by several simulation tests carried out on LV and MV distribution systems under different fault condition and DG size and location for grid-connected and islanded modes of operation. The simulation results show the protection method is selective with appropriate speed, and the protection settings are independent of the distribution system modes of operation.**

***Index Terms*— distribution system, distributed generation, communication-less protection, voltage-based relay.**

I. Introduction

PROTECTION of distribution system (DS) with distributed generation (DG) is a complex problem due to some issues including DG interface technology, daily change of DG output, and DS grid-connected or islanded (stand-alone) operational mode.

Depending on the interface technology, DG units make different fault current contribution. The fault contribution of the synchronous-based DG (SBDG) can reach up to several times of its nominal current, whilst for the inverter-based DG (IBDG) it is between 0.5-2 per-unit (p.u.) depending on the inverter controller [1-3].

The second issue is the daily change in the DG output, which can lead to change in the magnitude and direction of fault currents. For example, solar power plants are out of service at nights or wind farms produce energy only when the wind blows. Moreover, in longer term, the DG penetration level may vary by adding new DG or by changing the size of existing DG.

The third issue arises following a fault or disturbance at the grid side, where the protection must isolate the DS to operate in the islanded mode [4]. The fault current magnitude in the grid-connected mode is much different from the islanded mode.

A brief review of protection methods for DS with DG is presented here. In [5, 6] two methods are described for control of fault current contribution of DG. In order to reduce the fault current contribution from SBDG or grid, the use of fault current limiter (FCL) is proposed in [7, 8]. The main issues for employing FCL are its impedance and transient behavior [9].

A non-communication overcurrent (OC) protection method based on the definite time relay is proposed in [10]. The method may take a long time for fault isolation in large DSs. An agent-based method using the definite time OC relays and communication between the relays is proposed in [2]. In [11] a communication-assisted protection method is proposed where OC and undervoltage relays are used for fault detection in grid-connected and islanded modes of DS, respectively. The methods of [12, 13] use a communication link between OC relays and control center. After any change in the DS configuration or in DG status, the relay settings are calculated and loaded in the relays. In [14-16] the optimal relay settings are achieved by solving the protection coordination problem.

A voltage-based protection method using communication link between relays and voltage measurement devices at DG terminals is proposed in [17]. A communication-assisted protection method based on the voltage harmonic content of IBDG output is proposed in [18]. Methods in [17, 18] are used for grid-connected operating mode of DS.

References [19-21] propose differential protection for DSs. Due to the large number and short length of lines and the need for communication, use of differential protection method is difficult and costly [4].

Reference [22] proposes a distance protection (DP). The main issues for the use of DP in DSs with DG include the short length of lines and infeed current effect on the calculated impedance due to change in DG size and location [23].

A non-standard relay characteristic is presented in [24] for meshed DS. Three non-standard characteristics for fuse saving strategy in DS with high DG penetration are presented in [9, 25, 26]. A non-communication protection method using a non-standard relay characteristic for radial and meshed DS with SBDG is presented in [4]. However, the effectiveness of the

submitted date for review: 05/15/2018.
S. Jamali and H. Borhani-Bahabadi are with the School of Electrical Engineering, Iran University of Science and Technology, Tehran, Iran (e-mail: sjamali@iust.ac.ir, h_borhani@elec.iust.ac.ir).

method in radial DS with IBDG is not addressed by the authors.

Most of the protection methods for DSs with DG which are presented in the literature are communication-based or communication-assisted methods requiring fast processing unit [5], hence they are more costly [27]. Moreover, these methods are vulnerable to communication failures [19, 27] and, therefore, the reliability of the communication link is an important parameter for these protection methods.

In order to address the above-mentioned problems, a robust protection system must be able to operate under different fault condition and DS operation. The DS protection system must be reliable with appropriate selectivity and stability features. This paper presents a protection method for DSs with DG using local voltage measurement. The proposed method is tested for the both grid-connected and islanded modes of operation for LV and MV distribution systems. The method can cope with different fault condition, DS operating mode, and different DG type, size and location.

The rest of this paper is organized as follows: The proposed method is presented in Section II. The test LV and MV distribution systems are described in Section III. The results and discussion are presented in Section IV. Finally, in Section V the conclusion is presented.

II. PROPOSED METHOD

In this paper, a novel voltage-based protection method for DSs with DG is presented. The method is communication-less, effective in the grid-connected and islanded modes of operation of DS. Because the presence of DG will affect the direction of the fault current, to have a proper operation of the protection system, the relays must be equipped with a directional element. The proposed method provides main and backup protection against different fault condition.

A. Relay characteristic

Independent of the DG type and fault condition, the closer a bus to the fault has lower voltage magnitude and the voltage magnitude raises by increasing the distance from the fault location. Fig. 1 shows a simple distribution system, with 4 buses. Suppose a fault occurs between buses B2 and B3, L23, and the fault location is varied from 1% to 99% of the line length from B2. The voltage magnitude of B3 and B4, V3 and V4, respectively, with different fault resistances, R_f, in the grid-connected operating mode is shown in Fig. 2 in the presence of IBDG and SBDG. As expected, independent of the fault condition and DG type, a closer bus to the fault location has a lower voltage magnitude. A similar behavior is expected in islanded mode of operation of DS. In Fig. 2, for a better visualization of voltage magnitudes and voltage differences, the scale of voltage magnitude (y-axis) is different in each subplot.

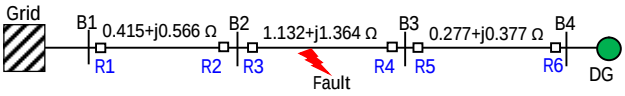

Fig. 1. A simple radial distribution system.

After analyzing the simulation results, it can be seen in Fig. 2 that the fault voltage magnitude in B3 and B4 is varied between less than 1% to more than 90% of nominal voltage, depending on the fault impedance and distance to the fault. The difference of fault voltage magnitude between the neighboring buses of B3 and B4 is also very low, in the range of less than 1%. Therefore, the proposed method must be able to operate under different fault condition which cause different fault voltage magnitude at relay locations. Also, the method must be able to create an appropriate coordination time interval while the difference of voltage magnitude between main and backup relays is very low.

The main idea for the proposed method is based on the fact that under any fault condition, a bus closer to the fault location has a lower voltage magnitude irrespective of the DS operating mode, as well as DG type, size and location.

Equations (1) and (2) gives the proposed voltage-based characteristic:

$$K = \left(\frac{V_{sc}}{2} \times \left(1 - \frac{V_{sc}}{2}\right)\right)^{m} \quad (1)$$

$$t = TDS \times \left(\frac{A}{\left(\frac{1}{K}\right)^{P} - 1}\right) \times Log_2\left(\frac{1}{K}\right) \times \left(\frac{1}{K}\right) + D \quad (2)$$

where t is the relay operating time, Vsc is the fault voltage

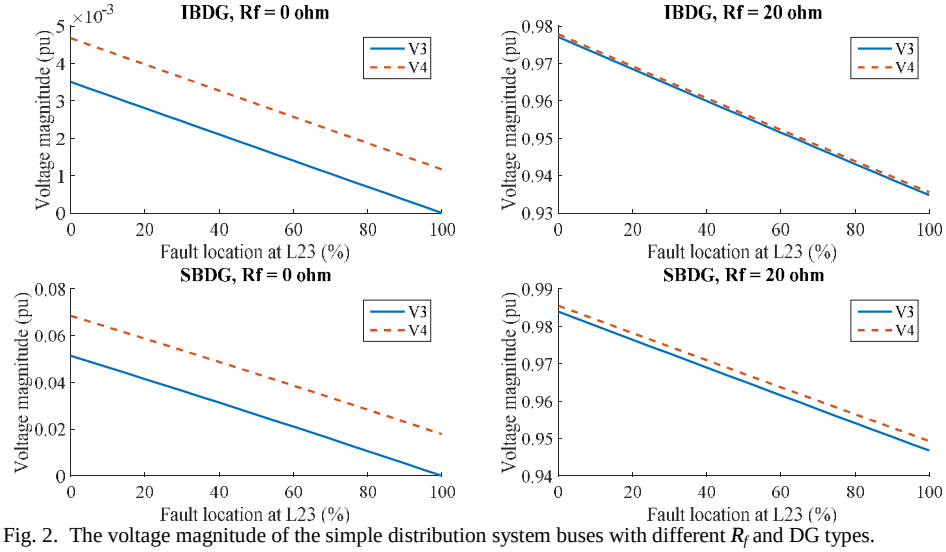

Fig. 2. The voltage magnitude of the simple distribution system buses with different R_f and DG types.

This article has been accepted for publication in a future issue of this journal, but has not been fully edited. Content may change prior to final publication. Citation information: DOI 10.1109/TPWRD.2018.2889895, IEEE Transactions on Power Delivery

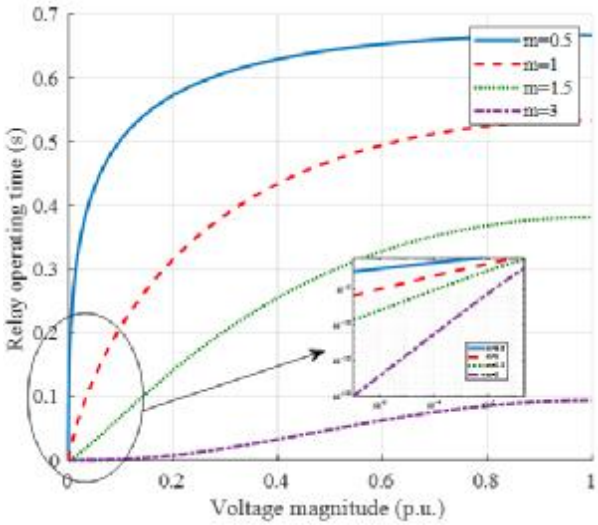

Fig. 3. The voltage-based characteristic curve.

magnitude in per-unit based on the nominal voltage of the system, *m*, *A*, *p* and *D* are the constant parameters; $Log_2(*)$ is the binary logarithm, and *TDS* is the time dial setting.

Fig. 3 illustrates the proposed characteristic curve for a relay with different values for *m*, *TDS=1*, *A*, *p* and *D* constants are set to 1, 2, and 0, respectively. The subplot in Fig. 3 shows logarithmic curves to improve visualization of the relay operating time for voltages lower than 0.1 per-unit.

The relay operating time with the proposed characteristic depends on the fault voltage magnitude at the relay location. Lower voltage magnitudes indicate a closer fault and hence the relay operating time must be smaller. It can be seen in Fig. 3 that with increasing fault voltage magnitude the relay operating time increases. Also, at very low fault voltages, because of steep slope of the relay characteristic, there is a considerable time difference between the fault voltages.

For a three-phase system, the tripping time is computed for each phases and the lower time is determined as the overall relay operating time to send to the related circuit breaker.

Two main settings for the proposed characteristic are *m* and *TDS*. Effect of the setting *m* on the relay characteristic and the tripping time is shown in Fig. 3, where the lower *m* setting leads to an increase in the slop of the characteristic.

TDS and *m* can be evaluated by using optimization methods [15, 16], in order to have same settings for both modes of DS operation. The next subsection provides a simple method for determination of these settings.

B. Determination of the relay setting

The proposed relay parameters include TDS, *m* and constant parameters. In this paper, *A* and *p* constants are set to 1 and 2, respectively. The value of *p* is considered 2 in accordance with the IEC extremely inverse characteristic, since the general standard form has been used. According to the presented characteristic, the value of *A* is multiplied by TDS. Therefore, its setting has a direct impact on the value of TDS. For simplicity, its value is considered one. *D* value is normally set to a non-zero value, e.g. between 0.03 and 0.08 seconds, which reflects, at least, the operation time of the circuit-breakers. It should, however, be noted that the constant parameters can be obtained using an optimization method such as the methods given in [15, 16].

In order to determine the TDS and *m* value for all the relays, at first, the *m* value is set to a single value between 0.1 and 3 for all the relays in the islanded mode. Then the TDS value is calculated by the following method. For the forward relays in grid-connected mode, the *m* value is set to a value between the value set in the islanded mode and 3, whilst the TDS values for grid-connected mode is fixed to the same value of the islanded mode. The reverse relays have the same settings in the both modes, i.e. the same as the islanded mode settings. The *m* value for forward relays in the grid-connected mode should satisfy the CTI requirement whilst the TDS of the relays remain unchanged. Because different *m* value is used for forward relays in grid-connected and islanded mode of operation, the relays are required to be equipped with islanding detection element.

In order to explain the TDS determination process, consider the radial system in Fig. 1. For a fault at B4, Relays R5, R3 and R1 are primary, backup1 and backup2, respectively. These relays are named as forward relays. For a fault at B1, Relays R2, R4 and R6 are primary, backup1 and backup2, respectively. These relays are named as reverse relays.

The coordination process is the same as overcurrent relays; with the difference that overcurrent relay TDSs are set for the network operating condition producing maximum fault currents [28], whereas in this paper the worst case is for network operating condition producing the maximum voltage drop following a fault condition. In order to have the maximum voltage drop, the DS should be in the islanded mode with inverter-based DG during a bolted fault.

For determining the TDS of forward relays the grid source is replaced with an IBDG in the islanded mode. For determining the TDS of reverse relays the IBDG is placed at the end of the feeder with the grid source is disconnected. The IBDG capacity is chosen to supply all the DS loads. A three-phase bolted fault is applied at the end of the feeder, B4, and the R5 operating time is calculated using the proposed characteristic. TDS of R5 is set to gain an acceptable minimum time. TDS of R4 is set in coordination with R5 with an appropriate coordination time interval (CTI). Similarly, the TDS of R1 is calculated. Using the same process, the TDS of reverse relays is determined.

C. The philosophy of using voltage

In the event of a short circuit in a DS, the short circuit current is supplied by sources, including the grid and DG. Depending on the respective location of the sources to the fault point, as well as the type of DG, the fault magnitude in each of the feed paths from the source can be very diverse. For example, currents up to several kA may flow from the grid path to the fault location, whereas the fault current of up to a few tens of amperes flow to the fault location from low-power SBDG or IBDG. The result of such an extreme difference in fault currents, which can also be caused by the change in the fault location, leads to the failure of maintaining the coordination of overcurrent relays. Therefore, in order to overcome the problem of large changes in fault current flow and lack of relay

This article has been accepted for publication in a future issue of this journal, but has not been fully edited. Content may change prior to final publication. Citation information: DOI 10.1109/TPWRD.2018.2889895, IEEE Transactions on Power Delivery

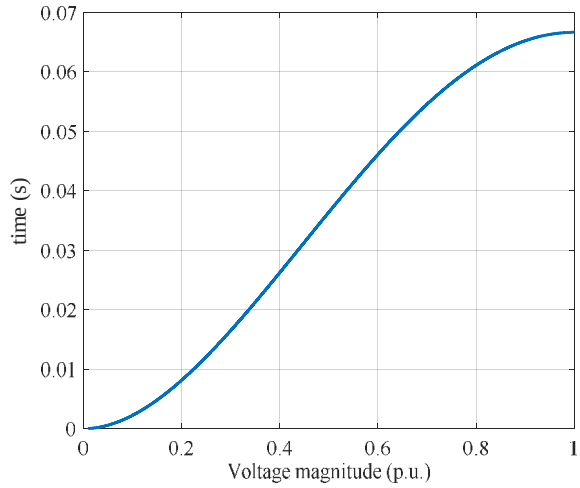

Fig. 4. IEC characteristic curve with (*1/Vsc*) instead of *Isc*.

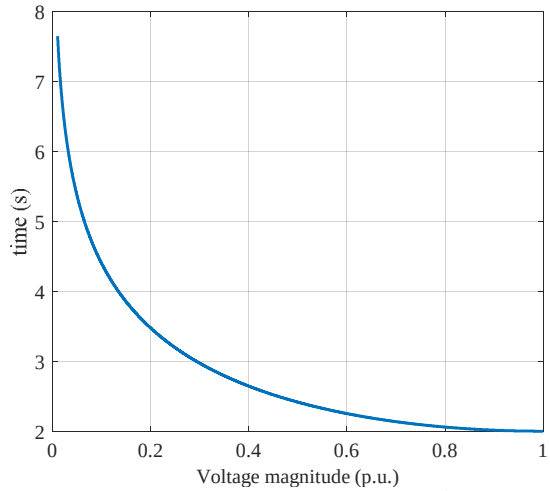

Fig. 5. Fuse characteristic curve with (*1/Vsc*) instead of *Isc*.

coordination, many methods have suggested the use of communication links.

On the other hand, a fault in a DS results in voltage drop in the system. By approaching the fault location, the voltage drop gets higher. In contrast to big changes in fault currents with respect to the fault location, the voltage magnitude can only change between 0 to 1 per-unit. Therefore, if a voltage-based characteristic can be found that can respond to small changes in the voltage magnitude during a fault, then it can be used for the relays coordination. The proposed characteristic in this paper has such a feature. The appearance of the proposed characteristic is in the form of a product of the standard IEC

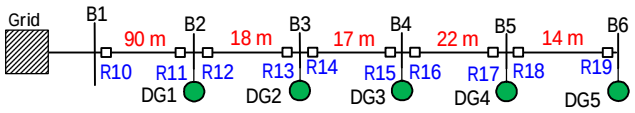

Fig. 6. The LV test distribution system.

standard time-current characteristic and the standard logarithmic overcurrent characteristic commonly used for fuses. The difference is that instead of using the current, the inverse per-unit voltage is used.

The IEC characteristic curve with (*1/Vsc*) instead of *Isc* is shown in Fig. 4. It is observed that the slope of the curve is positive but very low at low voltages. On the other hand, the characteristic of the fuse, with (*1/Vsc*) instead of *Isc* which is shown in Fig. 5, has a very high negative slope at low voltages. By multiplying these two curves together, a characteristic is obtained (Fig. 3) which has a sharp slope at very low voltages that can produce a discrimination time difference between the buses with low voltages. The relay settings for coordination is done under solid faults, therefore, the CTI can be achieved by setting the appropriate TDS. On the other hand, for low impedance faults, which result in the increase of the fault voltage magnitude, due to the increase of the relay operation time, relay coordination can be achieved by the selected TDS.

Thus, according to Fig. 3, the proposed characteristic has the feature for establishing the coordination between the system relays.

III. Test Systems

This section describes the LV and MV distribution test systems which are practical Iranian DSs used to validate the proposed voltage-based protection method.

The LV-DS has a nominal voltage of 0.4 kV with 6 buses, five DG and 10 directional relays as shown in Fig. 6. Type of line conductor is aluminum, 150 mm^2 with 0.207+j0.072 ohm/km impedance. The line lengths of L12, L23, L34, L45 and L56 are 90, 18, 17, 22 and 14 meters, respectively. A 10 kVA load with 0.85 lagging power factor is connected to each busbar, except B1. The LV-DS is supplied by an 11/0.4 kV, 630 kVA Dyn transformer with 4% transient reactance. The fault level at 11 kV busbar is 5.52 kA.

The second test DS is the 20 kV system shown in Fig. 5. The grid supply of the DS is from two 63/20 kV, YnD1, 30MVA transformers connected at B00. The fault current level at 63 kV busbar is 3.65 kA. The MV-DS is equipped with 13 directional proposed relays (R1 to R13). The detailed information of the MV-DS is given in [9]. In Fig. 7, points F1 to F8 represent fault locations. The candidate buses for the DG connection to the DS

TABLE I
Different Scenarios for the LV Distribution System for the Grid-Connected and Islanded Modes

Scenario	DG status	Each DG size, kVA	Each DG type	Scenario	DG status	Each DG size, kVA	Each DG type
1*	0, 0, 0, 0, 1	-	-	7	0, 1, 0, 1, 0	0, 40, 0, 40, 0	×, IB, ×, SB, ×
2	at B01	70	IB	8	1, 0, 1, 0, 1	30, 0, 30, 0, 30	SB, ×, IB, ×, IB
3	0, 0, 0, 0, 1	70	IB	9	1, 1, 1, 1, 1	15	IB
4	1, 0, 0, 1, 1	25	IB	10	1, 1, 1, 1, 1	15	SB
5	1, 0, 0, 1, 1	25	SB	11	1, 1, 1, 1, 1	15	IB, SB, IB, SB, IB
6	0, 1 , 1, 1, 0	0, 30, 30, 30, 0	×, IB, SB, SB, ×	12	1, 1, 1, 1, 1	15	SB, IB, SB, IB, SB

* only for the grid-connected mode of operation

This article has been accepted for publication in a future issue of this journal, but has not been fully edited. Content may change prior to final publication. Citation information: DOI 10.1109/TPWRD.2018.2889895, IEEE Transactions on Power Delivery

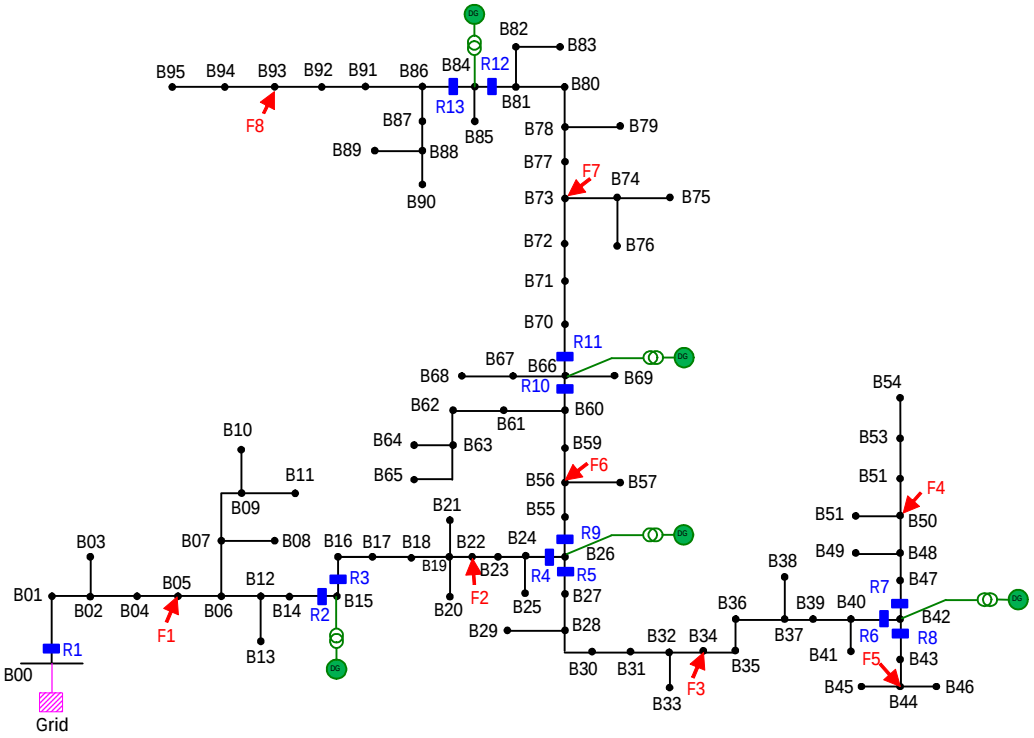

Fig. 7. The MV test distribution system with candidate buses for DG connection.

are B15, B26, B42, B66 and B84.

DG are directly connected to the LV-DS and in the MV-DS they are connected by 0.4/20 kV step-up transformer with 3% transient reactance.

The operating condition of the two DSs is different. The LV-DS has short line lengths and relays are installed at each line end, whereas in the MV-DS the relays are installed for protection of each zone consisting of several lines. Only one relay is used for the outer zone of the MV-DS. These test systems represent two extreme cases where DG in the LV-DS are close to each other and in the MV-DS are quite far from each other. Therefore, various scenarios in simulation study are carried out to evaluate the proposed method.

IV. Simulation Results and Discussion

A set of bolted three-phase faults (LLL) and single and double phase to earth faults (LLG and LG) are applied at the midpoint of each line in the LV-DS and at selected points, F1-F8, in the MV-DS.

In the simulation study, the fault current contribution of the IBDG is equal to its nominal current.

Various simulation scenarios are carried out on the LV- and MV-DS for both DS operating modes, different DG size and location under different fault condition. The appropriate CTI is taken as 0.2 seconds.

It is assumed that the islanded mode is occurred by opening the associated circuit breakers of R10 in the LV-DS and R1 in the MV-DS. Therefore, in the islanded mode, the relay at the head of feeder will not be a primary or backup protection.

A. Coordination results for the LV distribution system

The twelve scenarios of Table I are considered for the LV-DS by changing in- and out-of-service status of the DG in grid-connected and islanded modes of operation. In all the scenarios, the DG can supply loads in the islanded mode. In the second column in Table I, DG status '0' means DG is out-of-service and '1' means DG is in-service. The sequence of status, size and type of DG in columns 2 to 4 are according to the DG number in Fig. 4.

The TDS value of the relays is obtained using the method described in subsection II-B based on the second and the third scenarios in the islanded mode. The *m* value is set at 2, 1.5, 1.3, 1.3 and 0.5 for the forward relays R10, R12, R14, R16 and R18, respectively, in the grid-connected mode, and is set at 0.5 for all the relays in the islanded mode as well as the grid-connected mode for the reverse relays. The faults are applied to different lines and TDS values are set to achieve the proper CTI. Table II shows the TDS value of the relays for the both grid-connected and islanded modes of operation. The A, p and *D* values are set at 1, 2 and 0.03, respectively, for all relays.

For brevity, Table III shows the simulation results for the 12th scenario of Table I. The results in Table III are for LLL, LLG and LG faults occurring at the mid-point of the selected lines.

The results show the relay settings are achieved by the proposed method ensuring proper coordination with the CTIs equal or greater than 0.2 s for different fault types in the both modes of operation. In Table III, CTI_{GC} and CTI_{IL} represents CTI value in the grid-connected and islanded mode of operation, respectively.

Sum of the operating time of the main relays in the LV-DS

TABLE II
TDS VALUE OF THE RELAYS OF THE LV DISTRIBUTION SYSTEM

Relay	TDS	Relay	TDS	Relay	TDS	Relay	TDS
R10	1.410	R13	0.722	R16	1.161	R19	2.423
R11	0.001	R14	1.730	R17	1.846		
R12	2.722	R15	1.420	R18	0.001		

This article has been accepted for publication in a future issue of this journal, but has not been fully edited. Content may change prior to final publication. Citation information: DOI 10.1109/TPWRD.2018.2889895, IEEE Transactions on Power Delivery

TABLE III
PRIMARY AND BACKUP RELAY OPERATING TIMES OF SCENARIO 12 OF THE LV DISTRIBUTION SYSTEM

Fault location	Fault type	Primary relays					backup relays					CTI_{GC} (s)	CTI_{IL} (s)
		Relay	Grid-connected Vsc (p.u.)	Grid-connected t (s)	Islanded Vsc (p.u.)	Islanded t (s)	Relay	Grid-connected Vsc (p.u.)	Grid-connected t (s)	Islanded Vsc (p.u.)	Islanded t (s)		
B02-B03	LLL	R12	0.071	0.156	0.002	0.453	R10	0.767	0.359	-	-	0.204	-
		R13	0.004	0.172	0.004	0.171	R15	0.010	0.417	0.010	0.417	0.246	0.246
	LLG	R12	0.072	0.158	0.006	0.667	R10	0.782	0.362	-	-	0.204	-
		R13	0.004	0.175	0.004	0.171	R15	0.011	0.428	0.010	0.415	0.253	0.244
	LG	R12	0.072	0.159	0.004	0.584	R10	0.780	0.362	-	-	0.203	-
		R13	0.004	0.179	0.004	0.169	R15	0.012	0.440	0.010	0.413	0.261	0.244
B03-B04	LLL	R14	0.060	0.145	0.002	0.307	R12	0.185	0.386	0.006	0.653	0.241	0.347
		R15	0.003	0.295	0.003	0.295	R17	0.008	0.496	0.008	0.496	0.200	0.201
	LLG	R14	0.060	0.146	0.006	0.430	R12	0.188	0.391	0.019	0.923	0.244	0.493
		R15	0.004	0.304	0.003	0.293	R17	0.008	0.505	0.008	0.494	0.200	0.201
	LG	R14	0.061	0.147	0.004	0.378	R12	0.188	0.392	0.012	0.817	0.245	0.439
		R15	0.004	0.315	0.003	0.293	R17	0.009	0.519	0.007	0.496	0.205	0.203
B05-B06	LLL	R18	0.040	0.030	0.003	0.030	R16	0.167	0.230	0.012	0.364	0.200	0.334
		R19	0.001	0.349	0.001	0.349	-	-	-	-	-	-	-
	LLG	R18	0.041	0.030	0.006	0.030	R17	0.168	0.230	0.025	0.442	0.200	0.412
		R19	0.001	0.366	0.001	0.346	-	-	-	-	-	-	-
	LG	R18	0.041	0.030	0.005	0.030	R18	0.169	0.231	0.019	0.412	0.201	0.381
		R19	0.002	0.382	0.001	0.352	-	-	-	-	-	-	-

under 12th scenario and different fault types is equal to 5.906 and 7.360 seconds in grid connected and islanded modes, respectively. The same time for backup relays are 9.843 and 10.980 seconds, respectively.

Similar results can be obtained for other scenarios.

B. Protection coordination for the MV distribution system

In order to validate the protection method in the MV-DS, several scenarios using different fault type and various DG type, size and location are carried out in the grid-connected and islanded modes of operation as shown in Table IV.

The TDS value of relays for the second, fourth and sixth scenarios are determined by using the method explained in subsection II-B. The *m* value is set at 1, for relays R1, R3 and set at 0.8 for other forward relays R5, R7, R8, R9, R11 and R13, respectively, in the grid-connected mode and is set at 0.5 for all the relays in the islanded mode as well as for the reverse relays in the grid-connected mode. Table V gives the TDS value of the relays for the MV-DS in both operating modes. The A, p and D values are set at 1, 2 and 0.03, respectively, for all relays.

For brevity, Table VI only shows the simulation results for the 18th scenario at the selected fault points. Table VII shows the results for the similar scenario whilst the fault resistance, R_f, is equal to 40-ohm. The results show the 0.2 seconds CTI constraint is satisfied for all the fault points under different fault types.

As can be seen from the results, the proposed method can achieve proper protection coordination in both modes of operation under different fault types and resistance. The relay settings given in Table V are the same for grid-connected and islanded modes of operation under different fault conditions. The relay operating time at various fault conditions is low for primary relays. The CTI is also satisfied for various fault condition and fault location in the both modes of operation. Therefore, the method has proper speed and selectivity.

TABLE V
TDS VALUE OF RELAYS FOR THE MV DISTRIBUTION SYSTEM

Relay	TDS	Relay	TDS	Relay	TDS	Relay	TDS
R1	1.504	R5	0.421	R9	0.792	R13	0.001
R2	0.001	R6	1.259	R10	0.904		
R3	1.298	R7	0.001	R11	0.449		
R4	0.452	R8	0.001	R12	1.526		

For high fault impedance of 40-ohm at F6, the minimum CTI between the relays R9 and R3 is not respected. As shown in Fig. 3, at high fault voltages, the changes in the relay operating time are very low in response to small variations of the voltage. Therefore, in this case, because the fault voltage is very close to 1 per-unit, the minimum CTI is not satisfied. It is worth mentioning that relay settings are also important in this situation. As can be seen, there is appropriate coordination between other fault locations and conditions.

Under bolted fault the sum of the operating time of the main relays in the MV-DS under 18th scenario and different fault types is equal to 11.177 and 8.838 seconds in grid connected

TABLE IV
DIFFERENT SCENARIOS FOR THE MV DISTRIBUTION SYSTEM FOR BOTH OPERATING MODES

Scenario	DG connection bus/es	DG size, MW	DG type	Scenario	DG connection bus/es	DG size, MW	DG type
1*	-	-		10	B15,B42	3, 3	IB, SB
2	B00	6	IB	11	B26,B66	3, 3	SB, IB
3	B26	6	SB	12	B26,B84	3, 3	SB, IB
4	B42	6	IB	13	B42,B84	4, 2	SB, SB
5	B66	6	SB	14	B26,B42, B66	1, 2, 3	SB, SB, IB
6	B84	6	IB	15	B26, B42, B66, B84	2, 1, 2, 2	SB, IB, SB, IB
7	B15, B26, B42	2, 2, 2	IB, SB, IB	16	B15, B26, B42, B66, B84	1, 2, 1, 1, 1	SB, SB, SB, SB, SB
8	B15, B42, B66	2, 2, 2	SB, IB, SB	17	B15, B26, B42, B66, B84	1, 2, 1, 1, 1	IB, IB, IB, IB, IB
9	B26, B66, B84	2, 2, 2	IB, SB, SB	18	B15, B26, B42, B66, B84	1, 2, 1, 1, 1	IB, SB, IB, SB, IB

* only for the grid-connected mode of operation

This article has been accepted for publication in a future issue of this journal, but has not been fully edited. Content may change prior to final publication. Citation information: DOI 10.1109/TPWRD.2018.2889895, IEEE Transactions on Power Delivery

and

TABLE VI
PRIMARY AND BACKUP RELAY OPERATING TIMES OF SCENARIO 18 OF THE MV DISTRIBUTION SYSTEM UNDER BOLTED FAULT CONDITION

Fault location	Fault type	Primary relays					backup relays					CTI_{GC}	CTI_{IL}
			Grid-connected		Islanded			Grid-connected		Islanded			
		Relay	Vsc (p.u.)	t (s)	Vsc (p.u.)	t (s)	Relay	Vsc (p.u.)	t (s)	Vsc (p.u.)	t (s)	(s)	(s)
F2	LLL	R3	0.259	0.425	0.003	0.257	R1	0.547	0.755	-	-	0.330	-
		R4	0.030	0.200	0.029	0.199	R6	0.037	0.530	0.037	0.528	0.330	0.329
							R10	0.056	0.429	0.054	0.426	0.229	0.227
	LLG	R3	0.292	0.524	0.059	0.610	R1	0.543	0.754	-	-	0.230	-
		R4	0.154	0.277	0.081	0.247	R6	0.276	0.787	0.138	0.705	0.510	0.458
							R10	0.286	0.576	0.152	0.523	0.299	0.276
	LG	R3	0.301	0.531	0.033	0.529	R1	0.533	0.750	-	-	0.219	-
		R4	0.145	0.275	0.057	0.230	R6	0.259	0.780	0.089	0.648	0.505	0.418
							R10	0.266	0.570	0.102	0.486	0.295	0.256
F4	LLL	R7	0.074	0.030	0.028	0.030	R5	0.462	0.255	0.166	0.264	0.225	0.234
	LLG	R7	0.124	0.030	0.072	0.030	R5	0.584	0.266	0.312	0.288	0.236	0.258
	LG	R7	0.126	0.030	0.053	0.030	R5	0.582	0.266	0.243	0.279	0.236	0.249
F6	LLL	R9	0.131	0.307	0.026	0.315	R3	0.420	0.516	0.030	0.515	0.209	0.200
							R6	0.138	0.705	0.033	0.515	0.398	0.200
		R10	0.013	0.295	0.012	0.293	R12	0.015	0.497	0.014	0.493	0.202	0.200
	LLG	R9	0.202	0.359	0.074	0.403	R3	0.485	0.633	0.111	0.697	0.274	0.294
							R6	0.298	0.795	0.123	0.690	0.436	0.287
		R10	0.125	0.506	0.062	0.438	R12	0.239	0.929	0.114	0.819	0.423	0.381
	LG	R9	0.200	0.357	0.052	0.372	R3	0.483	0.632	0.071	0.636	0.275	0.264
							R6	0.282	0.789	0.079	0.632	0.432	0.260
		R10	0.103	0.488	0.037	0.389	R12	0.196	0.901	0.062	0.719	0.413	0.330
F8	LLL	R13	0.136	0.030	0.050	0.030	R11	0.267	0.236	0.098	0.255	0.206	0.225
	LLG	R13	0.291	0.030	0.162	0.031	R11	0.415	0.264	0.220	0.291	0.234	0.260
	LG	R13	0.285	0.030	0.113	0.031	R11	0.410	0.263	0.165	0.279	0.233	0.248

islanded modes, respectively, and the same time for backup relays are 20.184 and 17.012 seconds, respectively. Also, when R_f = 40-ohm, the sum of the operating time of main relays is 16.582 and 15.289 seconds in grid connected and islanded modes, respectively, whereas the same times for backup relays are 23.135 and 22.769 seconds, respectively.

Similar results can be obtained for other scenarios.

C. *Relay starter element*

It can be seen in Table VII that the voltage magnitude at relay location is very close to the voltage magnitude under normal operating condition. Therefore, a relay starter element is required to activate the proposed relay when the voltage magnitude is within the nominal voltage range (0.9 -1.1 p.u.).

In the simulation results, if the fault voltage at a relay

TABLE VII
PRIMARY AND BACKUP RELAY OPERATING TIMES OF SCENARIO 18 OF THE MV DISTRIBUTION SYSTEM WITH RF = 40-OHM

Fault location	Fault type	Primary relays					backup relays					CTI_{GC}	CTI_{IL0}
			Grid-connected		Islanded			Grid-connected		Islanded			
		Relay	Vsc (p.u.)	t (s)	Vsc (p.u.)	t (s)	Relay	Vsc (p.u.)	t (s)	Vsc (p.u.)	t (s)	(s)	(s)
F2	LLL	R3	0.993	0.617	0.919	0.895	R1	0.995	0.832	-	-	0.215	-
		R4	0.996	0.331	0.926	0.331	R6	1.000	0.869	0.930	0.869	0.538	0.538
							R10	1.002	0.633	0.926	0.632	0.302	0.301
	LLG	R3	1.001	0.617	1.030	0.895	R1	0.998	0.832	-	-	0.215	-
		R4	1.011	0.331	1.035	0.331	R6	1.023	0.869	1.046	0.869	0.538	0.538
							R10	1.023	0.632	1.038	0.632	0.301	0.301
	LG	R3	0.998	0.617	0.962	0.895	R1	0.997	0.832	-	-	0.215	-
		R4	1.004	0.331	0.967	0.331	R6	1.009	0.869	0.971	0.869	0.538	0.538
							R10	1.010	0.632	0.967	0.632	0.301	0.301
F4	LLL	R7	0.957	0.031	0.892	0.031	R5	0.990	0.280	0.922	0.311	0.249	0.280
	LLG	R7	0.982	0.031	1.001	0.031	R5	1.014	0.280	1.032	0.311	0.249	0.280
	LG	R7	0.976	0.031	0.939	0.031	R5	1.001	0.280	0.963	0.311	0.249	0.280
F6	LLL	R9	0.992	0.499	0.928	0.558	R3	0.994	0.617	0.928	0.895	0.118	0.337
							R6	0.996	0.869	0.933	0.869	0.370	0.311
		R10	0.989	0.632	0.920	0.632	R12	0.990	1.047	0.915	1.047	0.415	0.415
	LLG	R9	1.011	0.499	1.038	0.558	R3	1.009	0.617	1.042	0.895	0.118	0.337
							R6	1.022	0.869	1.048	0.869	0.370	0.311
		R10	1.010	0.632	1.029	0.632	R12	1.016	1.047	1.030	1.047	0.415	0.415
	LG	R9	1.001	0.499	0.969	0.558	R3	1.000	0.617	0.970	0.895	0.118	0.337
							R6	1.006	0.869	0.973	0.869	0.370	0.311
		R10	1.000	0.633	0.962	0.632	R12	1.003	1.047	0.958	1.047	0.414	0.415
F8	LLL	R13	0.970	0.031	0.893	0.031	R11	0.980	0.296	0.909	0.329	0.265	0.298
	LLG	R13	0.994	0.031	0.999	0.031	R11	1.006	0.296	1.017	0.330	0.265	0.299
	LG	R13	0.985	0.031	0.936	0.031	R11	0.994	0.296	0.950	0.330	0.265	0.299

This article has been accepted for publication in a future issue of this journal, but has not been fully edited. Content may change prior to final publication. Citation information: DOI 10.1109/TPWRD.2018.2889895, IEEE Transactions on Power Delivery

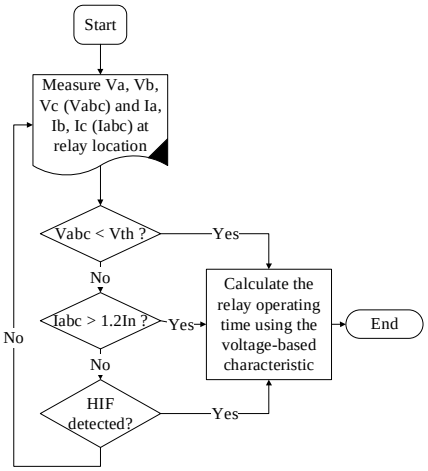

Fig. 8. The relay starter flowchart

location is less than a voltage threshold (Vth) value, 0.85 p.u., the fault can be detected by the undervoltage element. In the MV-DS case study, the fault current for R_f = 20-ohm is within the range of 1.5-2.5 times greater than the maximum normal load current, whilst the fault current during R_f = 40-ohm is very close to or less than the normal load current. Hence when the fault current is more than 1.2 times of the maximum normal load current, the fault can be detected by an overcurrent element. The 40-ohm fault resistance can be categorized as a high impedance fault (HIF), which can be detected by a HIF detector such as the method proposed in [29]. The flowchart of the starter element procedure is shown in Fig. 8.

D. Dynamic analysis

In this subsection, performance of proposed protection method is analyzed with the oscillography showing the voltage behavior at a bus in which the relay is connected.

In the grid-connected mode of operation of MV-DS, suppose a bolted LLL fault is occurring at F6. Relays R9 and R10 are primary relays. R3 and R6 are the backup relays for R9 and R12 is the backup relay for R10. Figure 9 shows the voltage oscillography of pre-fault voltage, fault voltage and post fault voltage at B26 and B66 as R9 and R10 location, respectively. Fault initiation and isolation times are also shown in Figs. 9 and 10. too. For the fault isolation, the responsible relay operates and isolates the fault. The fault clearing times are the same as the related results of Table VI.

In order to evaluate the backup relay operation time, R9 and R10 are disabled in the simulation study. Figure 10 shows the voltage oscillography at B15, B42 and B84 as the location of R3, R6 and R12, respectively.

By comparing the fault isolation times in Figs. 9 and 10, CTI can be evaluated.

E. Comparative analysis

A comparison of the protection methods mentioned in Section I, in terms of advantages and disadvantages including cost is presented in Table VIII. For the proposed voltage-based method, one voltage transformer (VT) connected at a bus can supply all the relays connected to that bus. For example, in Fig. 5 the VT at B42 can supply all the three relays R4, R5 and R9.

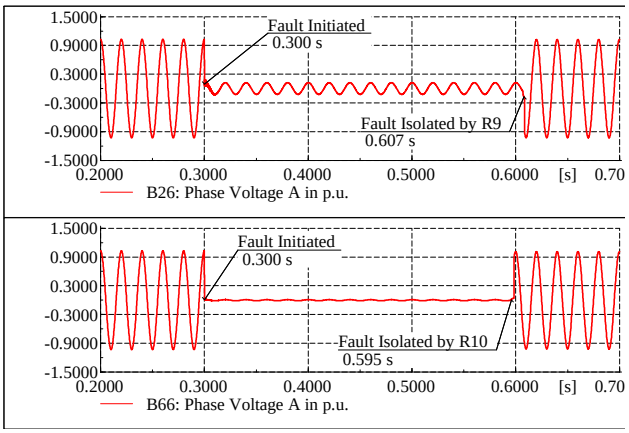

Fig. 9. Voltage oscillography at B26 and B66 during an LLL fault at F6.

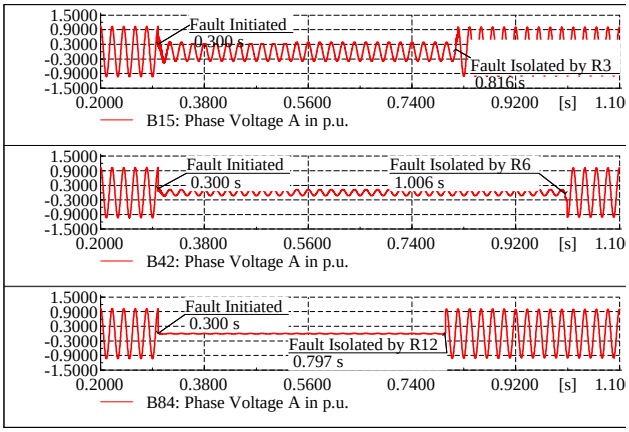

Fig. 10. Voltage oscillography at B15, B42 and B84 during an LLL fault at F6.

Furthermore, as explained for the relay starter element, each relay needs current transformer (CT). The cost view advantage of the proposed method is its communication-less feature.

V. Conclusion

This paper proposes a new voltage-based relay characteristic that can be used in DSs with DG. The proposed relay has two main settings: *m* and TDS. The TDS setting for all the relays in a DS are the same in both grid-connected and islanded modes of operation. The *m* value is the same for all the relays in the islanded mode, whereas for the grid-connected mode only the *m* value of the forward relays is changed to satisfy the CTI constraint. The method is validated by simulation study on LV and MV distribution system under different DG size and location, fault condition and DS mode of operation. The results show that the method is selective with appropriate speed under different fault scenarios. The highlights of the proposed method are as follows:

1) A communication-less method;

2) Uses only the local voltage magnitude measurement for determining the relay operating time;

3) Correct operation under all fault conditions in both grid-connected and islanded operating modes;

4) Use of the same settings for both modes of operation;

5) Independence of the DG type, size and location;

6) Use of a simple and low calculation algorithm.

TABLE VIII
COMPARISON OF THE DISTRIBUTION SYSTEM PROTECTION METHODS

Protection method	Ref.	Advantages	Disadvantages	Cost
Limiting the fault current contribution from DG or grid	[5-8]	Unchanged in DS fault level, no need to change protection settings	Not applicable for small IBDG and islanded mode and transient behaviour of DG must be checked.	High
Communication-based Overcurrent	[11-13]	Fast fault clearing time, immune against change in DG size and location,	Requires fast and reliable communication. In case of communication failure, needs an alternative protection system.	High
Voltage-based	[17,18]	Suitable for detection of faulted zone.	Requires fast and reliable communication. In case of communication failure, need an alternative protection system. Not used for the islanded mode. In absent of DG cannot operate. Dependence to DG type.	Relatively high
Differential	[19-21]	Fast fault clearing time, Independent of DN mode of operation	Requires fast and reliable communication. In case of communication failure, need an alternative protection system. A large number of relays is needed.	High
Proposed voltage-based method	-	Reliable method as it is communication-less, selective and fast, same setting for both operating modes, independent of DG type and fault condition	Requires protective VT, in addition to CT for the relays	Relatively low

REFERENCES

[1] M.H. Bollen, F. Hassan, "Integration of distributed generation in the power system," John Wiley & Sons; 2011, pp. 299-366.

[2] M.H. Cintuglu, T. Ma, O.A. Mohammed, "Protection of autonomous microgrids using agent-based distributed communication," IEEE Trans. Power Del., vol. 32, no. 1, pp. 351-360, 2017.

[3] H. Muda, P. Jena, "Sequence currents based adaptive protection approach for DNs with distributed energy resources," IET Gener. Transm. Distrib., vol. 11, no.1, pp.154-165, 2017.

[4] S. Jamali, H. Borhani-Bahabadi, "Non-communication protection method for meshed and radial distribution networks with synchronous-based DG," Int. J. Electr. Power Energy Syst., vol. 93, pp. 468-478, 2017.

[5] H. Yazdanpanahi, X. Wilsun, L. Yun Wei, "A novel fault current control scheme to reduce synchronous DG"s impact on protection coordination," IEEE Trans. Power Del., vol. 29, no. 2, pp. 542-551, 2014.

[6] M.I. Mosaad, N.I. Elkalashy, M.G. Ashmawy, "Integrating adaptive control of renewable distributed Switched Reluctance Generation and feeder protection coordination," Electr. Power Syst. Res., vol. 154, pp. 452-462, 2018.

[7] W. Rebizant, K. Solak, B. Brusilowicz, et al., "Coordination of overcurrent protection relays in networks with superconducting fault current limiters," Int. J. Electr. Power Energy Syst., vol. 95, pp. 307-314, 2018.

[8] K. Wheeler, M. Elsamahy, S. Faried, "Use of superconducting fault current limiters for mitigation of distributed generation influences in radial distribution network fuse–recloser protection systems," IET Gener. Transm. Distrib., vol. 11, no. 7, pp. 1605-1612, 2017.

[9] S. Jamali, H. Borhani-Bahabadi, "Recloser time-current-voltage characteristic for fuse saving in distribution networks with DG," IET Gener. Transm. Distrib., vol. 11, no. 1, pp. 272-279, 2017.

[10] M.A. Zamani, T.S. Sidhu, A. Yazdani, "A protection strategy and microprocessor-based relay for low-voltage microgrids," IEEE Trans. Power Del., vol. 26, no. 3, pp. 1873-1883, 2011.

[11] M.A. Zamani, A. Yazdani, T.S. Sidhu, "A communication-assisted protection strategy for inverter-based medium-voltage microgrids," IEEE Trans. Smart Grid, vol. 3, no. 4, pp. 2088-2099, 2012.

[12] M.Y. Shih, A. Conde, Z. Leonowicz, et al., "An adaptive overcurrent coordination scheme to improve relay sensitivity and overcome drawbacks due to distributed generation in smart grids," IEEE Trans. Ind. Appl., vol. 53, no. 6, pp. 5217-5228, 2017.

[13] F. Coffele, C. Booth, A. Dysko, "An adaptive overcurrent protection scheme for distribution networks," IEEE Trans. Power Del., vol. 30, no. S2, pp. 561-568, 2015.

[14] H.H. Zeineldin, H.M. Sharaf, D.K. Ibrahim, et al., "Optimal protection coordination for meshed distribution systems with DG using dual setting directional over-current relays," IEEE Trans. Smart Grid, vol. 6, no. 1, pp.115-123, 2015.

[15] K.A. Saleh, H.H. Zeineldin, E.F. El-Saadany, "Optimal protection coordination for microgrids considering N-1 contingency," IEEE Trans Ind. Informat., vol. 13, no. 5, pp. 2270-2278, 2017.

[16] A. Tjahjono, D.O. Anggriawan, A.K. Faizin, et al., "Adaptive modified firefly algorithm for optimal coordination of overcurrent relays," IET Gener. Transm. Distrib., vol. 11, no. 10, pp. 2575-2585, 2017.

[17] H. Al-Nasseri, M.A. Redfern, F. Li, "A voltage based protection for micro-grids containing power electronic converters," IEEE Power Engineering Society General Meeting; Montreal, Canada, pp. 1-7, June 2006.

[18] H. Al-Nasseri, M.A. Redfern, "Harmonics content based protection scheme for micro-grids dominated by solid state converters," 12th Int. Middle-East Power System Conf.; Aswan, Egypt, pp. 50-56, March 2008.

[19] H. Gao, J. Li, B. Xu, "Principle and implementation of current differential protection in distribution networks with high penetration of DGs," IEEE Trans. Power Del., vol. 32, no. 1, pp. 565-574, 2017.

[20] E. Casagrande, W.L. Woon, H.H. Zeineldin, et al., "A differential sequence component protection scheme for microgrids with inverter-based distributed generators," IEEE Trans. Smart Grid, vol. 5, no. 1, pp. 29-37, 2014.

[21] S.F. Zarei, M. Parniani, "A comprehensive digital protection scheme for low-voltage microgrids with inverter-based and conventional distributed generations," IEEE Trans. Power Del., vol. 32, no. 1, pp.441-452, 2017.

[22] A. Sinclair, D. Finney, D. Martin, et al., "Distance protection in distribution systems, how it assists with integrating distributed resources," IEEE Trans. Ind. Appl., vol. 50, no. 3, pp. 2186-2196, 2014.

[23] J. Kennedy, P. Ciufo, A. Agalgaonkar, "A review of protection systems for distribution networks embedded with renewable generation," Renewable and Sustainable Energy Rev., vol. 58, pp. 1308-1317, 2016.

[24] K.A. Saleh, H.H. Zeineldin, A. Al-Hinai, et al., "Optimal coordination of directional overcurrent relays using a new time-current-voltage characteristic. IEEE Trans. Power Del., vol. 30, no. 2, pp. 537-544, 2015.

[25] S. Jamali, H. Borhani-Bahabadi, "New recloser characteristic to improve fuse saving in distribution networks with distributed generation," Rev. Roum. Sci. Techn.– Électrotechn. et Énerg., vol. 62, no. 3, pp. 240-245, 2017.

[26] S. Jamali, H. Borhani-Bahabadi, "Self-adaptive relaying scheme of reclosers for fuse saving in distribution networks with DG," Int. J. Power Energy Res., vol. 1, no. 1, pp. 8-19, 2017.

[27] T.S. Ustun, R.H. Khan, "Multiterminal hybrid protection of microgrids over wireless communications network," IEEE Trans. Smart Grid, vol. 6, no. 5, pp. 2493-2500, 2015.

[28] ALSTOM. "Network Protection & Automation Guide," ALSTOM; 2002.

[29] A. Soheili, J. Sadeh, R. Bakhshi, "Modified FFT based high impedance fault detection technique considering distribution non-linear loads: simulation and experimental data analysis," Int. J. Electr. Power Energy Syst., vol. 94, pp. 124-140, 2018.